Research Article Vol. 58, No. 18 / 20 June 2019 / Applied Optics 4939

applied optics

Method for calculation and analysis of the weights of grating mosaic errors

Guojun Yang,[1,2] Xiangdong Qi,[1,*] Xiaotian Li,[1] Haili Yu,[1] Min Cong,[1,2] Xiaotao Mi,[1] and Shuo Yang[1]

[1]Grating Technology Laboratory, Changchun Institute of Optics, Fine Mechanics and Physics, Chinese Academy of Sciences, Changchun, Jilin 130033, China
[2]University of Chinese Academy of Sciences, Beijing 100049, China
*Corresponding author: chinagrating@263.net

Received 30 January 2019; revised 10 May 2019; accepted 27 May 2019; posted 28 May 2019 (Doc. ID 358787); published 14 June 2019

A method to calculate the weight of grating mosaic errors is proposed based on an analytical hierarchy process. An accurate mosaic error tolerance calculation formula is also presented that is useful for large-size grating fabrication by the mosaic method. The grating mosaic error weights and tolerances are analyzed for mosaic echelle gratings. The analytical error weight and tolerance results agree well with the experimental results. The mosaic grating's far-field intensity is 95.8%, which is higher than the 94% value from the simulation results.

https://doi.org/10.1364/AO.58.004939

1. INTRODUCTION

Large-sized diffraction gratings are important optical elements in numerous fields including astronomical telescopes, where they are used to improve spectral resolution [1–3], and petawatt-scale chirped-pulse lasers, where they are used to increase the laser output energy [4–6]. At present, the demand for large-sized diffraction gratings is becoming increasingly strong following the start-up of projects for the Thirty Meter Telescope (TMT) [7] and the 12 meter astronomical telescope in China [8]. The mosaic method, which is the main method used in large-sized diffraction grating fabrication, involves placing two or more relatively small-sized gratings together, adjusting their attitudes and their relative positional relationships, and rectifying the five-dimensional errors that occur between the gratings until the error tolerance requirements are met. The question of whether the mosaic grating meets the designed requirements is mainly dependent on whether the mosaic error meets the error tolerance. Therefore, calculation of the error tolerance becomes a decisively significant step for tiling of the gratings.

There are two methods that can be utilized to calculate the error tolerance: analysis of the far-field intensity distribution and analysis of the wavefront variation of the mosaic grating. Harimoto *et al.* calculated the tolerances of the rotation error around the grating vector direction θ_x, the rotation error around the grating line direction θ_y, and the horizontal shift error based on 90% of the bright ring energy in the far-field spot center of the zero-error mosaic grating and the formula for the far-field intensity distribution [9]. Qiao *et al.* calculated the tolerances of θ_x, θ_y, and the horizontal shift error based on a Monte Carlo tolerance analysis and the curves for the Strehl ratio and R80 with errors [10]. R80 is the radius of a circle inside which 80% of the total focused beam energy is enclosed. Cotel *et al.* calculated the tolerances for θ_x, θ_y, and the horizontal shift error based on the peak intensity, the pulse synchronization, and the pulse duration related to the constant, linear, and quadratic phase defaults, respectively [11]. Lu *et al.* calculated the tolerances for the five-dimensional errors based on 80% of the bright ring energy in the far-field spot center of the zero-error mosaic grating and the minimum change curve for the five-dimensional errors of the mosaic grating [12]. All the researchers noted above calculated the error tolerances based on the far-field intensity distribution of the grating. However, there no scholars have calculated the mosaic error tolerance based on the wavefront change of mosaic grating.

There is a calculation method for the error tolerance based on the wavefront variation of the grating, where the limit value of the error is multiplied by the weight factor of the error. This method can meet the requirements for arbitrary grating wavefront accuracy and far-field light intensity for mosaic gratings. Among these requirements, the limit value for the mosaic error can be calculated based on the relationship between the grating mosaic error and the wavefront, but the weight has not been calculated by many researchers.

In this work, the calculation model used for the weight of the mosaic error is established based on the analytic hierarchy process (AHP) [13–15], and an accurate formula to calculate the mosaic error tolerance is presented. Finally, the error weight and tolerance are analyzed for mosaic echelle gratings, and the calculation model used for the weight of the mosaic error is verified experimentally.

2. CALCULATION OF ERROR WEIGHT AND ERROR TOLERANCE FOR MOSAIC GRATING

A. Calculation of the Error Weight

Depending on the type of mosaic error and the effect of that mosaic error on the mosaic grating wavefront, there are five-dimensional mosaic errors that occur between the mosaic gratings when fabricating large-sized diffraction gratings using the mosaic method. These are as follows:

$$\begin{pmatrix} \textit{Rotation error around grating vector direction} \\ \textit{Rotation error around grating line direction} \\ \textit{Rotation error around the normal direction of grating} \\ \textit{Translation error along grating vector direction} \\ \textit{Translation error along the normal direction of grating} \end{pmatrix} = \begin{pmatrix} \Delta\theta_x \\ \Delta\theta_y \\ \Delta\theta_z \\ \Delta x \\ \Delta z \end{pmatrix}. \tag{1}$$

There are different difficulties during the five-dimensional errors that are corrected. The difficulty of error correction can be reduced by determining the influence of mosaic error on the wavefront of the mosaic grating and adjusting the tolerance of error. Therefore, it is highly important to calculate the weight of each of the five-dimensional errors for grating mosaics and provide a reasonable error tolerance calculation formula.

The specific process for calculation of the mosaic error weight involves establishing a hierarchical structure model of the error based on the error type and then building a hierarchical comparison matrix based on the ratios of these errors to obtain a normalized eigenvector. Finally, the dimensional error weighting matrix is built, and the error weights are calculated.

1. Establishment of a Hierarchical Structure Model for Mosaic Errors

Based on the various types of dimensional errors, the five-dimensional errors that occur between mosaic gratings can be divided into rotation errors $\Delta\theta$, which are denoted by $\Delta\theta_x$, $\Delta\theta_y$, and $\Delta\theta_z$, and translation errors ΔL, which are denoted by Δz and Δx as shown in Table 1.

2. Establishment of a Comparison Matrix for Different Levels of Mosaic Error

There are three-scale and nine-scale methods that can be used to construct a comparison matrix based on the user's subjective judgment in the traditional AHP [16]. This method involves uncertainty in the establishment of a pair comparison matrix for the grating mosaic errors. Therefore, the work in this paper establishes an error comparison matrix directly based on the ratios of each of the errors to build a more accurate error judgment matrix.

Table 1. Structural Model of the Mosaic Error

A	Mosaic Error				
B	Rotation error ($\Delta\theta$)			Translation error (ΔL)	
C	$\Delta\theta_x$	$\Delta\theta_y$	$\Delta\theta_z$	Δx	Δz

The error hierarchical structure model presented in Table 1 indicates that the weight comparison matrix A-B for the rotation error ($\Delta\theta$) and translation error (ΔL) relative to overall mosaic error; the weight comparison matrix $B_1 - C$ for the $\Delta\theta_x$, $\Delta\theta_y$, and $\Delta\theta_z$ error relative to overall rotation error ($\Delta\theta$); and the weight comparison matrix $B_2 - C$ for the Δx and Δz error relative to overall translation error (ΔL) can be expressed as

$$A - B = \begin{pmatrix} 1 & \frac{\Delta\theta}{\Delta L} \\ \frac{\Delta L}{\Delta\theta} & 1 \end{pmatrix}, \tag{2}$$

$$B_1 - C = \begin{pmatrix} 1 & \frac{\Delta\theta y}{\Delta\theta z} & \frac{\Delta\theta x}{\Delta\theta z} \\ \frac{\Delta\theta z}{\Delta\theta y} & 1 & \frac{\Delta\theta x}{\Delta\theta y} \\ \frac{\Delta\theta z}{\Delta\theta x} & \frac{\Delta\theta y}{\Delta\theta x} & 1 \end{pmatrix}, \tag{3}$$

$$B_2 - C = \begin{pmatrix} 1 & \frac{\Delta x}{\Delta z} \\ \frac{\Delta z}{\Delta x} & 1 \end{pmatrix}. \tag{4}$$

The eigenvectors of Eqs. (2)–(4) are calculated and normalized as follows:

$$E_0 = \begin{pmatrix} \frac{\Delta\theta}{\Delta L+\Delta\theta} \\ \frac{\Delta L}{\Delta L+\Delta\theta} \end{pmatrix}, \tag{5}$$

$$E_1 = \begin{pmatrix} \frac{\Delta\theta x\cdot\Delta\theta y}{\Delta\theta x\cdot\Delta\theta y+\Delta\theta x\cdot\Delta\theta z+\Delta\theta y\cdot\Delta\theta z} \\ \frac{\Delta\theta x\cdot\Delta\theta z}{\Delta\theta x\cdot\Delta\theta y+\Delta\theta x\cdot\Delta\theta z+\Delta\theta y\cdot\Delta\theta z} \\ \frac{\Delta\theta y\cdot\Delta\theta z}{\Delta\theta x\cdot\Delta\theta y+\Delta\theta x\cdot\Delta\theta z+\Delta\theta y\cdot\Delta\theta z} \end{pmatrix}, \tag{6}$$

$$E_2 = \begin{pmatrix} \frac{\Delta x}{\Delta x+\Delta z} \\ \frac{\Delta z}{\Delta x+\Delta z} \end{pmatrix}. \tag{7}$$

3. Calculation of the Weight for Each Dimensional Error Relative to the Total Error

According to Eqs. (5)–(7), the weight distribution matrix V, which is composed of factors at each level relative to the factors at the upper level, and the weight distribution matrix M of the factors at the upper level relative to the overall objective can be expressed as

$$V = \begin{pmatrix} \frac{\Delta\theta x\cdot\Delta\theta y}{\Delta\theta x\cdot\Delta\theta y+\Delta\theta x\cdot\Delta\theta z+\Delta\theta y\cdot\Delta\theta z} & 0 \\ \frac{\Delta\theta x\cdot\Delta\theta z}{\Delta\theta x\cdot\Delta\theta y+\Delta\theta x\cdot\Delta\theta z+\Delta\theta y\cdot\Delta\theta z} & 0 \\ \frac{\Delta\theta y\cdot\Delta\theta z}{\Delta\theta x\cdot\Delta\theta y+\Delta\theta x\cdot\Delta\theta z+\Delta\theta y\cdot\Delta\theta z} & 0 \\ 0 & \frac{\Delta x}{\Delta x+\Delta z} \\ 0 & \frac{\Delta z}{\Delta x+\Delta z} \end{pmatrix}, \tag{8}$$

$$M = E_0 = \begin{pmatrix} \frac{\Delta\theta}{\Delta L+\Delta\theta} \\ \frac{\Delta L}{\Delta L+\Delta\theta} \end{pmatrix}. \tag{9}$$

Therefore, the weight matrix P of the five-dimensional errors between mosaic gratings can be obtained by multiplying the weight distribution matrix V by the weight distribution matrix M, and the weight matrix P of the five-dimensional errors between mosaic gratings can be then expressed as

$$P = \begin{pmatrix} \frac{\Delta\theta x\cdot\Delta\theta y}{\Delta\theta x\cdot\Delta\theta y+\Delta\theta x\cdot\Delta\theta z+\Delta\theta y\cdot\Delta\theta z}\cdot\frac{\Delta\theta}{\Delta L+\Delta\theta} \\ \frac{\Delta\theta x\cdot\Delta\theta z}{\Delta\theta x\cdot\Delta\theta y+\Delta\theta x\cdot\Delta\theta z+\Delta\theta y\cdot\Delta\theta z}\cdot\frac{\Delta\theta}{\Delta L+\Delta\theta} \\ \frac{\Delta\theta y\cdot\Delta\theta z}{\Delta\theta x\cdot\Delta\theta y+\Delta\theta x\cdot\Delta\theta z+\Delta\theta y\cdot\Delta\theta z}\cdot\frac{\Delta\theta}{\Delta L+\Delta\theta} \\ \frac{\Delta x}{\Delta x+\Delta z}\cdot\frac{\Delta L}{\Delta L+\Delta\theta} \\ \frac{\Delta z}{\Delta x+\Delta z}\cdot\frac{\Delta L}{\Delta L+\Delta\theta} \end{pmatrix}. \tag{10}$$

In Eq. (10), $\Delta\theta = \Delta\theta_x + \Delta\theta_y + \Delta\theta_z$ and $\Delta L = \Delta x + \Delta z$.

The relationships between the mosaic error and the diffraction wavefront can be expressed as follows [17]:

$$\Delta_{\mathrm{OPD}} = (-y\cdot\Delta\theta_x + x\cdot\Delta\theta_y + \Delta z)(\cos\alpha + \cos\beta) + (y\cdot\Delta\theta_z + \Delta x)\cdot\frac{m\lambda}{d}. \tag{11}$$

In Eq. (11), α is the angle of incidence, β is the diffraction angle, d is the grating constant, m is the diffraction order, λ is the wavelength of the detection light, and Δ_{OPD} is the optical path difference between the mosaic gratings. y is oriented parallel to the grating line direction, and x is oriented parallel to the grating vector direction.

According to Eq. (11), the maximum optical path difference can be expressed as follows:

$$\Delta_{\mathrm{OPD\ max}} = (-L\cdot\Delta\theta_x + W\cdot\Delta\theta_y + \Delta z)(\cos\alpha + \cos\beta) + (L\cdot\Delta\theta_z + \Delta x)\cdot\frac{m\lambda}{d}. \tag{12}$$

In Eq. (12), L is the grating length along the grating line and W is the grating width along the grating vector direction.

Therefore, when the five-dimensional errors exist separately, the limit value of the five-dimensional errors between the mosaic gratings can be expressed as follows:

$$\begin{pmatrix} \Delta\theta_{x\ \max} \\ \Delta\theta_{y\ \max} \\ \Delta\theta_{z\ \max} \\ \Delta x_{\max} \\ \Delta z_{\max} \end{pmatrix} = \begin{pmatrix} \frac{\Delta_{\mathrm{OPD\ max}}}{L(\cos\alpha+\cos\beta)} \\ \frac{\Delta_{\mathrm{OPD\ max}}}{W(\cos\alpha+\cos\beta)} \\ \frac{\Delta_{\mathrm{OPD\ max}}}{L(\sin\alpha+\sin\beta)} \\ \frac{\Delta_{\mathrm{OPD\ max}}}{(\sin\alpha+\sin\beta)} \\ \frac{\Delta_{\mathrm{OPD\ max}}}{(\cos\alpha+\cos\beta)} \end{pmatrix}. \tag{13}$$

Finally, according to Eq. (13), Eq. (10) becomes

$$P = \begin{pmatrix} \frac{L\cdot c\cdot a^2+d\cdot a\cdot b}{L\cdot(c+d)\cdot a^2+[c^2+d\cdot(1+c+L)]a\cdot b+c\cdot(d+W)\cdot b^2} \\ \frac{W\cdot c\cdot a\cdot b+W^2\cdot b^2}{L\cdot(c+d)\cdot a^2+[c^2+d\cdot(1+c+L)]a\cdot b+c\cdot(d+W)\cdot b^2} \\ \frac{L\cdot c\cdot a\cdot b+d\cdot b^2}{L\cdot(c+d)\cdot a^2+[c^2+d\cdot(1+c+L)]a\cdot b+c\cdot(d+W)\cdot b^2} \\ \frac{d\cdot b}{(c+d)\cdot a+(W+d)\cdot b} \\ \frac{d\cdot a}{(c+d)\cdot a+(W+d)\cdot b} \end{pmatrix}. \tag{14}$$

In Eq. (14), $a = \sin\alpha + \sin\beta$, $b = \cos\alpha + \cos\beta$, $c = L + W$, and $d = L\cdot W$. Additionally, only the numerical calculation of the corresponding parameters is considered in the weight calculation process.

B. Calculation of Error Tolerance

In Eq. (14), a larger value for each dimensional error weight in matrix P means that the error has a greater influence on the mosaic grating wavefront. To meet the wavefront accuracy requirements of the mosaic grating, the corresponding error tolerance should be reduced. Therefore, when calculating the weight factor for the five-dimensional errors, the corresponding weight of each error should be first subtracted from 1 and then normalized. The weight factor for each dimensional error relative to the total error can be defined as ε. ε indicates the proportion of five-dimensional mosaic errors under the premise of satisfying the wavefront requirements of the mosaic grating, and the sum of the weight factors of the five-dimensional errors is 1. The weight factor ε for each dimensional error relative to the total error can be calculated as

$$\begin{pmatrix} \varepsilon_{\Delta\theta x} \\ \varepsilon_{\Delta\theta y} \\ \varepsilon_{\Delta\theta z} \\ \varepsilon_{\Delta x} \\ \varepsilon_{\Delta z} \end{pmatrix} = \begin{pmatrix} \frac{1-P_{\Delta\theta x}}{4} \\ \frac{1-P_{\Delta\theta y}}{4} \\ \frac{1-P_{\Delta\theta z}}{4} \\ \frac{1-P_{\Delta x}}{4} \\ \frac{1-P_{\Delta z}}{4} \end{pmatrix}. \tag{15}$$

In Eq. (15), $P_{\Delta\theta x}$, $P_{\Delta\theta y}$, $P_{\Delta\theta z}$, $P_{\Delta x}$, and $P_{\Delta z}$ are the weights of the five-dimensional errors calculated in Eq. (14), respectively. The sum of $P_{\Delta\theta x}$, $P_{\Delta\theta y}$, $P_{\Delta\theta z}$, $P_{\Delta x}$, and $P_{\Delta z}$ is 1.

The error tolerance of the mosaic grating can be calculated as the limit value for the five-dimensional errors between the mosaic gratings multiplied by the corresponding weight factor for each dimensional error relative to the total error. Finally, the error tolerance of the mosaic grating can be calculated as

$$\begin{pmatrix} \Delta\theta x \\ \Delta\theta y \\ \Delta\theta z \\ \Delta x \\ \Delta z \end{pmatrix} = \begin{pmatrix} \Delta\theta x_{\max}\cdot\varepsilon_{\Delta\theta x} \\ \Delta\theta y_{\max}\cdot\varepsilon_{\Delta\theta y} \\ \Delta\theta z_{\max}\cdot\varepsilon_{\Delta\theta z} \\ \Delta x_{\max}\cdot\varepsilon_{\Delta x} \\ \Delta z_{\max}\cdot\varepsilon_{\Delta z} \end{pmatrix} = \begin{pmatrix} \frac{\Delta}{L\cdot b}\cdot\frac{L\cdot d\cdot a^2+[c^2+d\cdot(L+c)]\cdot a\cdot b+c\cdot(d+W)\cdot b^2}{4\cdot[L\cdot(c+d)\cdot a^2+[c^2+d\cdot(1+c+L)]\cdot a\cdot b+c\cdot(d+W)\cdot b^2]} \\ \frac{\Delta}{W\cdot b}\cdot\frac{L\cdot(c+d)\cdot a^2+[c^2-W^2+d\cdot(L+c)]\cdot a\cdot b+d\cdot(1+c)\cdot b^2}{4\cdot[L\cdot(c+d)\cdot a^2+[c^2+d\cdot(1+c+L)]\cdot a\cdot b+c\cdot(d+W)\cdot b^2]} \\ \frac{\Delta}{L\cdot a}\cdot\frac{L\cdot(c+d)\cdot a^2+[c^2-L^2+d\cdot(L+c)]\cdot a\cdot b+(c\cdot d+W^2)\cdot b^2}{4\cdot[L\cdot(c+d)\cdot a^2+[c^2+d\cdot(1+c+L)]\cdot a\cdot b+c\cdot(d+W)\cdot b^2]} \\ \frac{\Delta}{a}\cdot\frac{L\cdot(c+d)\cdot a^2+[c^2+d\cdot(1+c)]\cdot a\cdot b+W\cdot c\cdot b^2}{4\cdot[L\cdot(c+d)\cdot a^2+[c^2+d\cdot(1+c+L)]\cdot a\cdot b+c\cdot(d+W)\cdot b^2]} \\ \frac{\Delta}{b}\cdot\frac{L\cdot c\cdot a^2+[c^2+d\cdot(1+L)]\cdot a\cdot b+c\cdot(d+W)\cdot b^2}{4\cdot[L\cdot(c+d)\cdot a^2+[c^2+d\cdot(1+c+L)]\cdot a\cdot b+c\cdot(d+W)\cdot b^2]} \end{pmatrix}. \tag{16}$$

3. WEIGHT AND TOLERANCE ANALYSIS OF EACH DIMENSIONAL ERROR

A. Weight Analyses of Each Dimensional Error

The mosaic gratings in this paper are mainly used in the astronomical field, and so are the echelle gratings [18,19]. Therefore, the parameter ranges of $45° < \alpha = \beta < 90°$ and $0\ \mathrm{mm} < L = W \le 500\ \mathrm{mm}$ can be set.

Equation (14) then becomes

$$P=\begin{pmatrix}\frac{2\cdot a^2+a\cdot b}{(2+L)\cdot a^2+(5+3L)\cdot a\cdot b+2\cdot(L+1)\cdot b^2}\\ \frac{2\cdot a\cdot b+b^2}{(2+L)\cdot a^2+(5+3L)\cdot a\cdot b+2\cdot(L+1)\cdot b^2}\\ \frac{2\cdot a\cdot b+b^2}{(2+L)\cdot a^2+(5+3L)\cdot a\cdot b+2\cdot(L+1)\cdot b^2}\\ \frac{L\cdot b}{(2+L)\cdot a+(1+L)\cdot b}\\ \frac{L\cdot a}{(2+L)\cdot a+(1+L)\cdot b}\end{pmatrix}. \quad (17)$$

In Eq. (17), $a=2\sin\alpha$ and $b=2\cos\alpha$. The weight of each dimensional error relative to the total error is related to the angle of incidence α and the size L of the mosaic grating element. Therefore, the weight change in each dimensional error relative to the total error is simulated using MATLAB based on Eq. (17).

Figure 1 shows that the weight of each dimensional error changes relative to the total error when α and L change. $P_{\theta x}>P_{\theta y}=P_{\theta z}>P_{\Delta z}>P_{\Delta x}$; the influence of $\Delta\theta_x$ on the wavefront of the mosaic grating is greatest, while the effects of $\Delta\theta_y$ and $\Delta\theta_z$ on the wavefront of the mosaic grating are equal, and the effects of Δz and Δx on the wavefront of the mosaic grating are the smallest. Therefore, the weight factor and the tolerance of the mosaic error can be adjusted based on the influence of the five-dimensional errors between the mosaic gratings on the mosaic grating wavefront, which can help reduce the difficulty involved in rectifying each dimensional error under the condition that the mosaic grating wavefront is ensured when the grating mosaic error is rectified. Adjustment of the error weight factor and the error tolerance can be performed by adjusting the value of the error weight.

2. Tolerance Analyses for Each Dimensional Error

The wavefront of mosaic gratings is mainly detected via self-collimating incidence on echelle gratings. The parameter ranges of $45°<\alpha=\beta<90°$ and $0\ \text{mm}<L=W\le 500\ \text{mm}$ can be set. Equation (16) then becomes

$$\begin{pmatrix}\Delta\theta x\\ \Delta\theta y\\ \Delta\theta z\\ \Delta x\\ \Delta z\end{pmatrix}=\begin{pmatrix}\frac{\Delta}{L\cdot b}\cdot\frac{L\cdot a^2+(4+3L)\cdot a\cdot b+2\cdot(L+1)\cdot b^2}{4\cdot[(2+L)\cdot a^2+(5+3L)\cdot a\cdot b+2\cdot(L+1)\cdot b^2]}\\ \frac{\Delta}{L\cdot b}\cdot\frac{(2+L)\cdot a^2+(3+3L)\cdot a\cdot b+(1+2L)\cdot b^2}{4\cdot[(2+L)\cdot a^2+(5+3L)\cdot a\cdot b+2\cdot(L+1)\cdot b^2]}\\ \frac{\Delta}{L\cdot a}\cdot\frac{(2+L)\cdot a^2+(3+3L)\cdot a\cdot b+(1+2L)\cdot b^2}{4\cdot[(2+L)\cdot a^2+(5+3L)\cdot a\cdot b+2\cdot(L+1)\cdot b^2]}\\ \frac{\Delta}{a}\cdot\frac{(2+L)\cdot a^2+(2+2L)\cdot a\cdot b+2\cdot b^2}{4\cdot[(2+L)\cdot a^2+(5+3L)\cdot a\cdot b+2\cdot(L+1)\cdot b^2]}\\ \frac{\Delta}{b}\cdot\frac{2\cdot a^2+(5+L)\cdot a\cdot b+2\cdot(L+1)\cdot b^2}{4\cdot[(2+L)\cdot a^2+(5+3L)\cdot a\cdot b+2\cdot(L+1)\cdot b^2]}\end{pmatrix}. \quad (18)$$

In Eq. (18), $a=2\sin\alpha$ and $b=2\cos\alpha$. The tolerance of each dimensional error is related to the angle of incidence α and the size L of each mosaic grating element. Therefore, the tolerance change for each dimensional error is simulated based on Eq. (18) using MATLAB.

Figure 2 shows that the tolerance of $\Delta\theta_y$ is greater when the angle of incidence is larger and the grating size is smaller; the tolerance of $\Delta\theta_x$ is higher when the angle of incidence is larger and the grating size is smaller; the tolerance of $\Delta\theta_z$ is lower when the grating size is larger; and the tolerances of Δz and Δx change very little when the angle of incidence and the grating size change. The tolerance of $\Delta\theta_y$ is the largest, the tolerance of $\Delta\theta_x$ is smaller than that of $\Delta\theta_y$, the tolerance of $\Delta\theta_z$ is smaller than that of $\Delta\theta_x$, the tolerance of Δz is smaller than that of $\Delta\theta_z$, and the tolerance of Δx is smaller than that of Δz. Figure 2 shows the sizes of the five-dimensional error tolerances, which can help in setting the precision for the mosaic device.

The parameters can be set such that $L=W=35$ mm, $\alpha=\beta=64°$, and $\Delta=\lambda/6$. Therefore, the error tolerance of the mosaic grating can be calculated using the error tolerance calculation formula provided in this paper. The error tolerances are $\Delta\theta_x=0.4332$ μrad, $\Delta\theta_y=0.6515$ μrad, $\Delta\theta_z=0.3177$ μrad, $\Delta x=14.5681$ nm, and $\Delta z=29.6584$ nm.

The error tolerance calculations can be verified by the quality of the mosaic grating. Two methods can be used to evaluate the quality of the mosaic grating: 1) detection of whether or not the mosaic grating wavefront meets the application requirements and 2) detection of whether or not the energy gathered within the central bright disk in the far-field pattern of the

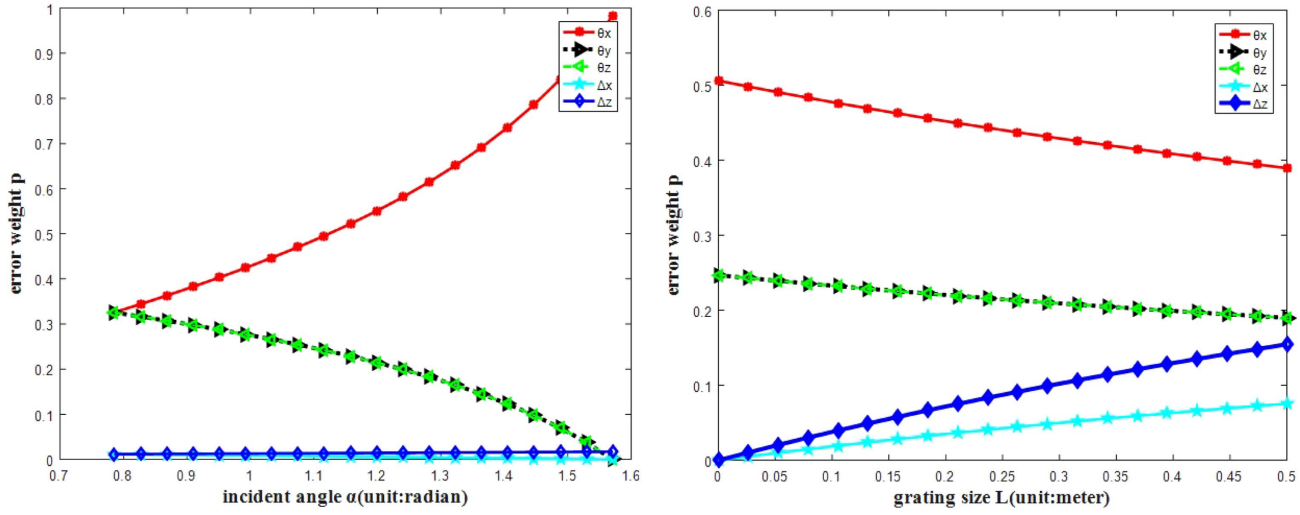

Fig. 1. (a) Weight variation curves for the mosaic errors versus incident angle α. (b) Weight variation curves for the mosaic errors versus grating size L.

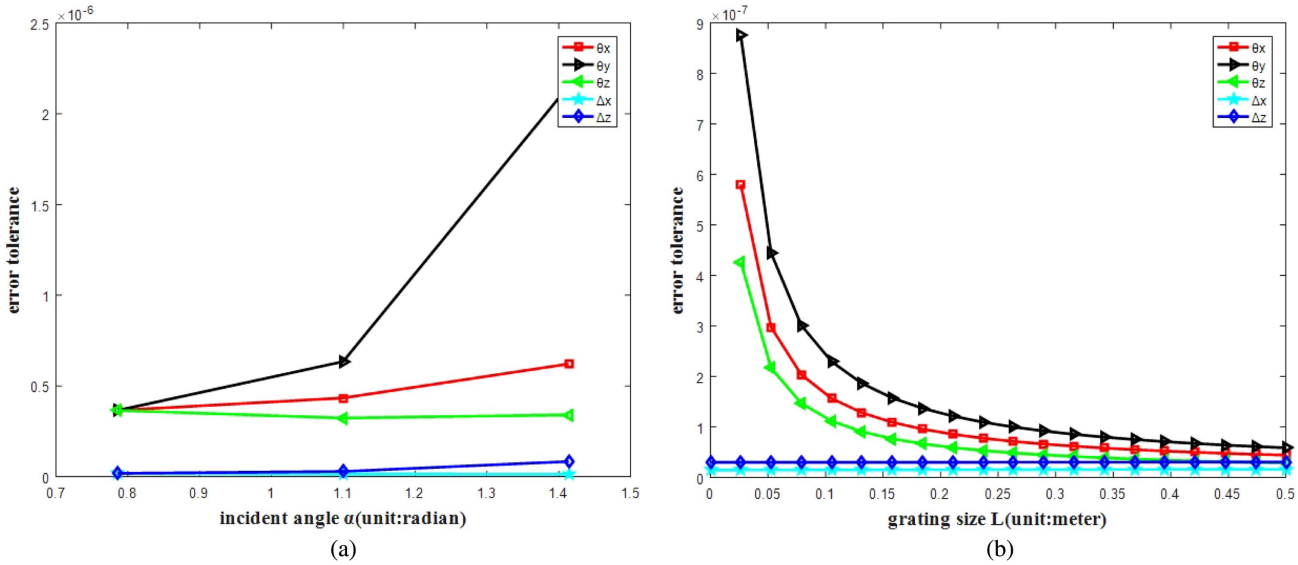

Fig. 2. (a) Variation curves of error tolerance versus incident angle α. (b) Variation curves of error tolerance versus grating size L.

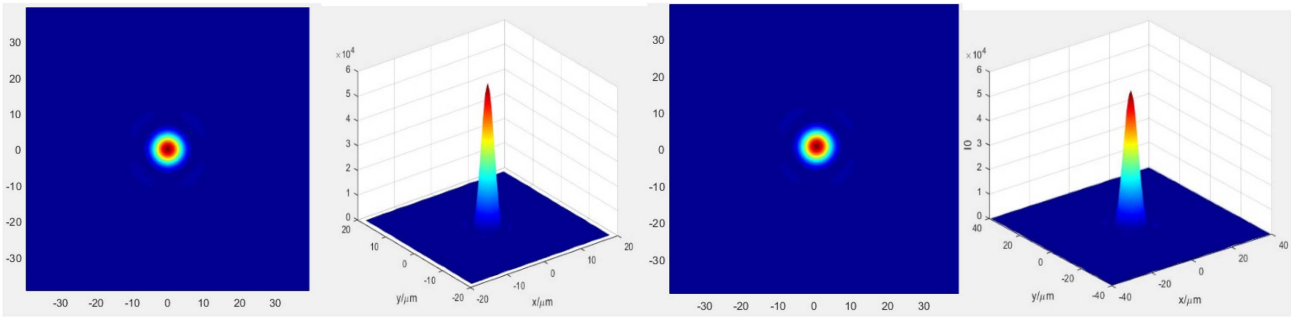

Fig. 3. (a1) and (b1) Far-field spot and intensity, respectively, for a mosaic grating with zero error. (a2) and (b2) Far-field spot and intensity, respectively, for a mosaic grating with $\Delta\theta_x = 0.4332$ μrad, $\Delta\theta_y = 0.6515$ μrad, $\Delta\theta_z = 0.3177$ μrad, $\Delta x = 14.5681$ nm, and $\Delta z = 29.6584$ nm.

mosaic grating is greater than or equal to 90% of the corresponding energy without errors [9]. In this paper, the error parameters in the tolerance calculation were obtained based on the mosaic grating wavefront. Therefore, the mosaic grating quality is more reasonably established using the second of these grating quality evaluation methods.

Figure 3 shows the far-field spot and the light intensity of the mosaic grating for the zero-error case and for the case of error tolerances of $\Delta\theta_x = 0.4332$ μrad, $\Delta\theta_y = 0.6515$ μrad, $\Delta\theta_z = 0.3177$ μrad, $\Delta x = 14.5681$ nm, and $\Delta z = 29.6584$ nm. The far-field light intensity of the mosaic grating is 94% of that of the zero-error case as shown in Fig. 3(b2). Therefore, the quality of the mosaic grating based on the values calculated in this paper meets the second evaluation criterion for the mosaic grating quality.

4. EXPERIMENTAL RESULTS

Figure 4(a) shows the mosaic device. The rotational accuracy of this device is 0.3 μrad, while the translation accuracy is 1 nm. First, the mosaic device is used to mosaic two gratings until the interference fringes on the surfaces of these two gratings are identical. For these mosaic gratings, the area is 35 mm× 70 mm, the groove density is 79 lines/mm, the blaze angle is 64°, and the mosaic order is 36. Figure 4(b) shows the Strehl ratio and the 36-order diffraction spot of the mosaic grating, where the Strehl ratio of the mosaic grating is 0.958. The mosaic grating's far-field intensity is 95.8% of that of the zero-error case, which is greater than the value of 94% obtained from the simulation results. The mosaic grating's far-field intensity matches the simulated results of Fig. 3 for the error tolerance. Figure 4(c) shows the wavefront of the mosaic grating. The peak-to-valley (PV) wavefront $= 0.513\lambda$ (where $\lambda = 632.8$ nm), and the root mean square (rms) wavefront $= 0.038\lambda$ ($\lambda = 632.8$ nm).

Additionally, the wavefront variation curve of the mosaic grating with the error is obtained using a Zygo interferometer to verify the simulation results for the error weight. The rotation and translation errors of the mosaic gratings are adjusted

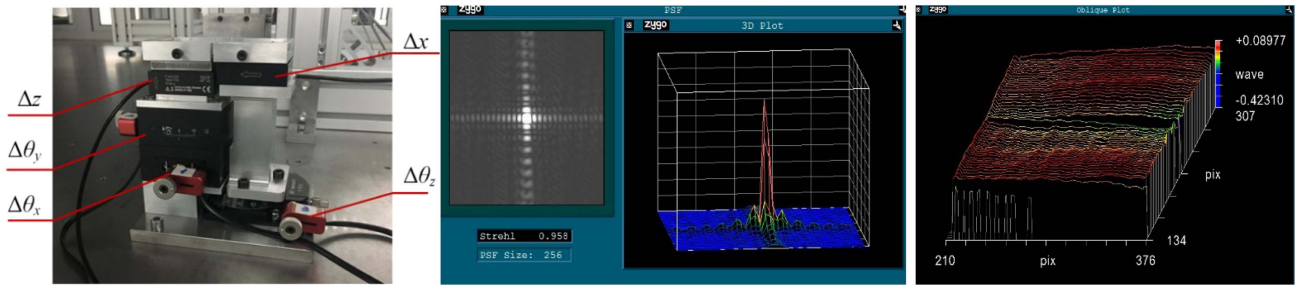

Fig. 4. (a) Mosaic device; (b) Strehl ratio and diffraction spot for the mosaic grating; (c) wavefront of the mosaic grating.

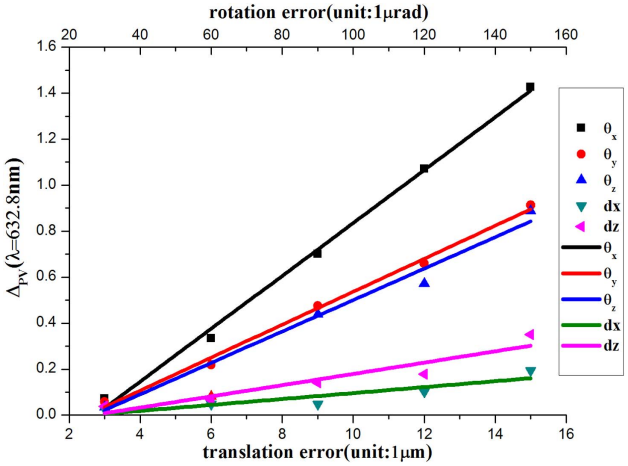

Fig. 5. Wavefront variation curve for the mosaic grating with errors.

separately to obtain the variation data for the PV wavefront. To make the mosaic grating wavefront change obvious, the rotation error and the translation error used for each adjustment are 30 μrad and 3 μm, respectively. Finally, ORIGIN software is used to provide a linear fit of the wavefront variation data for the mosaic grating.

Figure 5 shows the wavefront variation curve for the mosaic grating with the error. Δ_{PV} represents the wavefront difference between the mosaic grating after each adjustment of the mosaic errors and the initial mosaic grating that meets the error tolerance. Here, $k_{\theta x} > k_{\theta y} \approx k_{\theta z} > k_{\Delta z} > k_{\Delta x}$, where k is the curve slope. The influence of $\Delta\theta_x$ on the mosaic grating wavefront is highest, while the effects of $\Delta\theta_y$ and $\Delta\theta_z$ on the mosaic grating wavefront are almost equal, and the effects of both Δz and Δx on the mosaic grating wavefront are smaller.

The wavefront variation curve with errors shows good agreement with the results of the error weight analysis. $k_{\theta x} > k_{\theta y} \approx k_{\theta z} > k_{\Delta z} > k_{\Delta x}$ relates to $P_{\theta x} > P_{\theta y} = P_{\theta z} > P_{\Delta z} > P_{\Delta x}$, which directly verifies the validity of establishing the error weight calculation model based on the AHP.

5. CONCLUSIONS

This paper presents a method to calculate the mosaic error weight and the mosaic error tolerance for mosaic gratings. The weights and tolerances of each of the dimensional errors in mosaic echelle gratings are analyzed using this method. It is concluded that the effect of rotation error is larger than that of translation error on the wavefront of mosaic grating, and it is concluded that the change of rotation error tolerance is larger than that of translation error tolerance with the change of incident angle and grating size.

The variation curve of the wavefront with errors was obtained using a mosaic of two diffraction gratings with dimensions of 35 mm × 35 mm, a groove density of 79 lines/mm, and a blaze grade of 36. The experimental results agree well with the results of the error weight analysis. Additionally, the mosaic grating's far-field intensity is 95.8%, which is greater than the value of 94% given by the simulation results. The experiments and simulations verified the calculations of the error weight and the error tolerance based on this model and also verified that this model meets the requirements for both arbitrary wavefront accuracy and far-field intensity.

The proposed model can calculate the error tolerance according to the wavefront requirements and can reduce the rectification difficulties for mosaic errors by adjusting the error tolerance based on the error weight. Therefore, the method used to calculate the mosaic error weight and the mosaic error tolerance is particularly useful in both cases: when the wavefront of the mosaic grating has a definite range and when the mosaic errors have different rectification difficulties.

Funding. National Natural Science Foundation of China (NSFC) (61505204, 61605204); Chinese Ministry of National Science and Technology Program (2016YFF0102006, 2016YFF0103304); Key Technological Research Project of Jilin Province (20190302047GX); National Youth Program Foundation of China (61805233); Jilin Province Outstanding Youth Project in China (20170520167JH, 20180520190JH).

REFERENCES

1. T. Sakanoi, Y. Kasaba, M. Kagitam, H. Nakagawa, J. Kuhn, and S. Okano, "Development of infrared echelle spectrograph and mid-infrared heterodyne spectrometer on a small telescope at Haleakala, Hawaii for planetary observation," Proc. SPIE **9147**, 91478D (2014).
2. N. Bonod and N. Jérôme, "Diffraction gratings: from principles to applications in high-intensity lasers," Adv. Opt. Photon. **8**, 156–199 (2016).
3. R. Jacob, B. Aaron, P. Kevin, and P. Jannick, "Freeform spectrometer enabling increased compactness," Light Sci. Appl. **6**, 1–10 (2017).

4. T. Kessler, J. Bunkenburg, H. Huang, A. Kozlov, and D. D. Meyerhofer, "Demonstration of coherent addition of multiple gratings for high-energy chirped-pulse-amplified laser," Opt. Lett. **29**, 635–637 (2004).
5. N. Blanchot, G. Marre, J. Neauport, E. Sibe, C. Rouyer, S. Montant, A. Cotel, C. Le, and C. Sauteret, "Synthetic aperture compression scheme for a multipetawatt high-energy laser," Appl. Opt. **45**, 6013–6021 (2006).
6. S. Breitkopf, T. Eidam, A. Klenke, L. Von, H. Carstens, S. Holzberger, E. Fill, T. Schreiber, F. Krausz, A. Tunnermann, I. Pupeza, and J. Limpert, "A concept for multiterawatt fibre lasers based on coherent pulse stacking in passive cavities," Light Sci. Appl. **3**, e211 (2014).
7. S. Warren, "Thirty Meter Telescope detailed science case: 2015," Res. Astron. Astrophys. **15**, 1945–2140 (2015).
8. X. Q. Cui, "China's large optical infrared telescope," in *Proceedings of Abstract Collection of the 16th National Optical Testing Academic Exchange Conference* (Academic, 2016), pp. 2.
9. T. Harimoto, "Far-field pattern analysis for an array grating compressor," Jpn. J. Appl. Phys. **43**, 1362–1365 (2004).
10. J. Qiao, A. Kalb, M. Guardalben, G. King, D. Canning, and J. Kelly, "Large-aperture grating tiling by interferometry for petawatt chirped-pulse-amplification systems," Opt. Express **15**, 9562–9574 (2007).
11. A. Cotel, M. Castaing, P. Pichon, and C. Blanc, "Phased-array grating compression for high-energy chirped pulse amplification lasers," Opt. Express **15**, 2742–2752 (2007).
12. Y. X. Lu, X. D. Qi, H. L. Yu, X. T. Li, S. W. Zhang, S. Jiang, and L. Yin, "Precision analysis of grating replicated mosaic error based on the principle of Fraunhofer," Chin. J. Laser **43**, 0508005 (2016).
13. T. B. I. Mano, G. Guillen-Gosalbez, L. Jimenez, and M. Ravagnani, "Synthesis of heat exchanger networks with economic and environmental assessment using fuzzy-analytic hierarchy process," Chem. Eng. Sci. **195**, 185–200 (2019).
14. T. L. Saaty, K. Peniwati, and J. S. Shang, "The analytic hierarchy process and human resource allocation: half the story," Math. Comput. Model. **46**, 1041–1053 (2007).
15. T. L. Saaty and L. G. Varagas, *Models, Methods, Concepts & Applications of the Analytic Hierarchy Process* (Kluwer Academic, 2001).
16. Z. Q. Luo and S. L. Yang, "Comparative study on several scales in AHP," Syst. Eng. Theor. Prac. **10**, 51–59 (2004).
17. Y. X. Lu, X. D. Qi, X. T. Li, H. L. Yu, S. Jiang, H. G. Bayan, and L. Yin, "Removal of all mosaic grating errors in a single-interferometer system by a phase-difference reference window," Appl. Opt. **55**, 7997–8002 (2016).
18. Y. T. Zhu, "High resolution spectrographs for 8–10 m class optical/IR telescopes," Prog. Astron. **19**, 336–345 (2001).
19. T. Blasiak and S. Zheleznyak, "History and construction of large mosaic diffraction gratings," Proc. SPIE **4485**, 370–377 (2002).